Chinese Journal of Chemistry, **2009**, *27*, 1871—1878 **Full Paper**

Theoretical Studies on the Structures, Thermodynamic Properties, Detonation Performance, and Pyrolysis Mechanisms for Six Dinitrate Esters

LI, Miaomiao*(李苗苗) GUO, Xiaode(郭效德) LI, Fengsheng(李凤生)
SONG, Hongchang(宋洪昌)

School of Chemical Engineering, Nanjing University of Science and Technology, Nanjing 210094, China

Density functional theory (DFT) has been employed to study the geometric and electronic structures of six dinitrate esters including ethylene glycol dinitrate (EGDN), diethylene glycol dinitrate (Di-EGDN), triethylene glycol dinitrate (Tri-EGDN), tetraethylene glycol dinitrate (Tetra-EGDN), pentaethylene glycol dinitrate (Penta-EGDN) and hexaethylene glycol dinitrate (Hexa-EGDN) at the B3LYP/6-31G* level. Their IR spectra were obtained and assigned by vibrational analysis. Based on the frequencies scaled by 0.96 and the principle of statistic thermodynamics, the thermodynamic properties were evaluated, which were linearly related with the number of CH_2CH_2O groups as well as the temperature, obviously showing good group additivity. Detonation performances were evaluated by the Kamlet-Jacobs equations based on the calculated densities and heats of formation. It was found that density, detonation velocity, detonation pressure decreased with the increase of the number of CH_2CH_2O groups. Thermal stability and the pyrolysis mechanism of the title compounds were investigated by calculating the bond dissociation energies (BDE) at the B3LYP/6-31G* level. For the nitrate esters, the O—NO_2 bond is a trigger bond during a thermolysis initiation process.

Keywords nitrate ester, density functional theory, thermodynamic property, pyrolysis mechanism, detonation performance

Introduction

Nitrate ester explosives are an interesting group of explosive systems. Historically nitrate esters have been used for oil well fracturing, inserting a break in a forest fire, mine field clearance, and liquid landmines. Nowadays, they are also used as plasticizer and as mono- or bi-propellants. Therefore, they have been receiving considerable attention and a lot of investigations. Their structures, heats of formation, bond dissociation energy, *etc*. have been the subjects of many experimental and theoretical investigations. However, previous studies were mainly focused on some famous nitrate ester explosives, such as pentaerythritol tetranitrate (PETN) and nitroglycerine (NG),[6-9] few literature involves the dinitrate ester explosives. To our knowledge, Turker and Zeng *et al*.[6-9] investigated the structural and electronic properties of ethylene glycol dinitrate, triethylene glycol dinitrate, and tetraethylene glycol dinitrate based on density functional theory (DFT), respectively. To date, few systematic theoretical studies on homologic dinitrate esters based on DFT have been performed. In this paper, the compounds, such as ethylene glycol dinitrate, diethylene glycol dinitrate, triethylene glycol dinitrate, tetraethylene glycol dinitrate, pentaethylene glycol dinitrate, hexaethylene glycol dinitrate (Figure 1) are fully optimized at the DFT-B3LYP/6-31G* level to obtain the molecular geometry, electronic structure, molecular volume (*V*), theoretical crystal density (ρ), detonation velocity (*D*) and detonation pressure (*P*), as well as the bond dissociation energy (BDE). In addition, the pyrolysis mechanism, thermal stability and sensitivity are also studied.

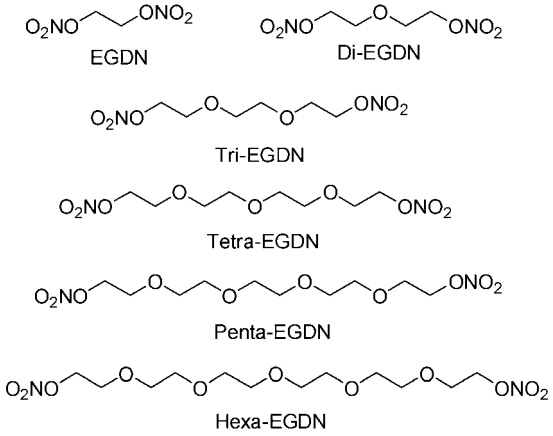

Figure 1 The molecular structures of EGDN, Di-EGDN, Tri-EGDN, Tetra-EGDN, Penta-EGDN and Hexa-EGDN.

* E-mail: miaomiao406@hotmail.com; Tel.: 0086-025-84315942; Fax: 0086-025-84315942
Received January 15, 2009; revised March 30, 2009; accepted May 12, 2009.

Computational methods

Many studies have shown that the DFT-B3LYP method in combination with the 6-31G* basis set is able to give the accurate energies, molecular structures, and infrared vibrational frequencies.[10-16] In this paper, six dinitrate esters were fully optimized to obtain their molecular geometries and electronic structures. Vibrational analyses were performed thereafter at the same level with the Gaussian 03 program package.[17] Since the DFT-calculated harmonic vibrational frequencies are usually larger than those observed experimentally, they were scaled using a factor of 0.96 as done before.[18] On the basis of the principle of statistical thermodynamics,[19] heat capacity, entropy, and enthalpy ranging from 200 to 800 K were derived from the scaled frequencies using a self-compiled program.

Detonation velocity (D), and detonation pressure (P) are the important parameters to evaluate the explosive performances of energetic materials. For the explosives with C, H, N and O elements, these parameters can be calculated using the Kamlet-Jacbos (K-J) equations:[20,21]

$$D = (1.011 + 1.312\rho_0)\,(N\overline{M}^{0.5}Q^{0.5})^{0.5} \quad (1)$$

$$P = 1.558\rho_0^2 N\overline{M}^{0.5}Q^{0.5} \quad (2)$$

where P is the detonation pressure (GPa), D is the detonation velocity (km/s), ρ_0 is the packed density (g/cm^3), N is the moles of gas produced by per gram of explosives, M is the average molar weight of detonation products, and Q is the chemical energy of detonation (kJ/g). Obviously, for known explosives, their Q and ρ_0 can be measured experimentally; thus their D and P can be calculated according to Eqs. (1) and (2). However, for those unsynthesized explosives and hypothetical compounds, their Q and ρ_0 cannot be evaluated from experimental measures. Therefore, in the molecular design of HEDC (high energy density compounds), in order to predict the detonation performance, we recommend the modified K-J equations based on the calculation results of quantum chemistry.[22-24]

In detail, the loading density of the explosives ρ_0 can be replaced by the theoretical crystal density (ρ_{cry}), while the chemical energy of the detonation reaction Q can be calculated as the difference between the heats of formation (E_{HOF}) of products and that of reactants (Q_{cal}). However, from the K-J equations, it is found that Q has much less effect than ρ_{cry} on D and P. Therefore, Q and E_{HOF} estimated using the semi-empirical MO PM3[25] method are precise enough to substitute the experimental data as has been proven in the previous studies.[26] Based on the ρ and Q, the corresponding D and P can be evaluated. In practice, ρ_0 can only approximate to but not arrive at ρ_{cry}, thus the D and P obtained from ρ_{cry} can be seen as their upper limit (maximum values).

As known to all, accurate prediction of crystal density is of large difficulty. The "group or volume additivity" method,[27,28] although simple and rapid, cannot give reliable results owing to its inherent drawbacks; while the "crystal packing" method,[29,30] which is more reliable, has its limitation in routine calculation due to its extensive requirement for computational resources. Recently, an efficient and convenient way has been worked out to predict the crystalline densities of energetic materials containing C, H, N and O elements.[31] Studies have indicated that when the average molar volume V estimated by the Monte-Carlo method based on 0.001 electron/bohr^3 density space at the B3LYP/6-31G** or 6-31G* level is used, the theoretical molecular density ρ_{mol} ($\rho_{mol} = M/V$, M being the molecular weight) is very close to the experimental crystal density ρ_{cry}. It is worthy noting that the average volume used here should be the statistical average of at least 100 volume calculations.

In a word, the modified K-J equation has been endowed with the new connotation and its application range has been extended. And on the basis of quantum chemistry, it has been used to calculate D and P to quantitatively evaluate HEDC in molecular design. The modified method has resulted in satisfactory results.

To measure the strength of bonds and relative stabilities of the title compounds, the bond dissociation energies (BDE) of various bonds in molecule are calculated. BDE is the required energy in homolysis of a bond and is commonly denoted by the difference between the total energies of the product and the reactant after zero-point energy correction. The expressions for the homolysis of A—B bond [Eq. (3)] and for calculating its BDE [Eq. (4)] are shown as follows:[32]

$$R_1A\text{-}BR_2(g) \rightarrow R_1A(g) + R_2B(g) \quad (3)$$

$$BDE_{(R_1A-BR_2)} = [E_{R_1A} + E_{R_2B}] - E_{(R_1A-BR_2)} \quad (4)$$

All the calculations considered here were performed on a Pentium IV personal computer using the default convergence criteria given in the programs.

Results and discussion

Infrared spectra and thermodynamic properties

As we all know, IR spectrum is one basic property of a compound, and also an effective measure to analyze or identify substances. Besides, it has a direct relation with the thermodynamic properties. Here, all the IR data (see the supporting information Figure 1S) of the title compounds were obtained at the DFT B3LYP/6-31G* level. From the IR spectra of the title compounds, it can be seen that there are six characteristic regions. In the range of 2860—3043 cm^{-1}, the modes are associated with the C—H symmetry and asymmetry stretching and the number of vibration equals to that of C—H bonds, *eg*., EGDN has four bands of 2962, 2983, 3025 and

3039 cm^{-1}. It is remarkable that, there are five very strong IR active modes. One is in the range of 1682—1700 cm^{-1}, corresponding to the NO_2 asymmetric stretching. Another is in the 1265—1295cm^{-1} range, arising from the NO_2 symmetry stretching. The third is located in the range of 1125—1145cm^{-1}, corresponding to the characteristic peaks of ether groups (CH_2CH_2O). The fourth is in the range of 1002—1034 cm^{-1}, corresponding to the C—O symmetry stretching. The last in the region less than 1000 cm^{-1} is the fingerprint region, which can be used to identify isomers, and the relatively strong peaks in this region are mainly caused by the O—NO_2 symmetry stretching. It is noticeable that, with the increase in CH_2CH_2O groups, the vibration intensity of ether groups increases obviously, *eg*., the intensity of ether groups of Hexa-EGDN is 1293.

To testify the reliability of theoretical computation, the calculated and experimental infrared spectra[33] of EGDN are compared (Figure 2).

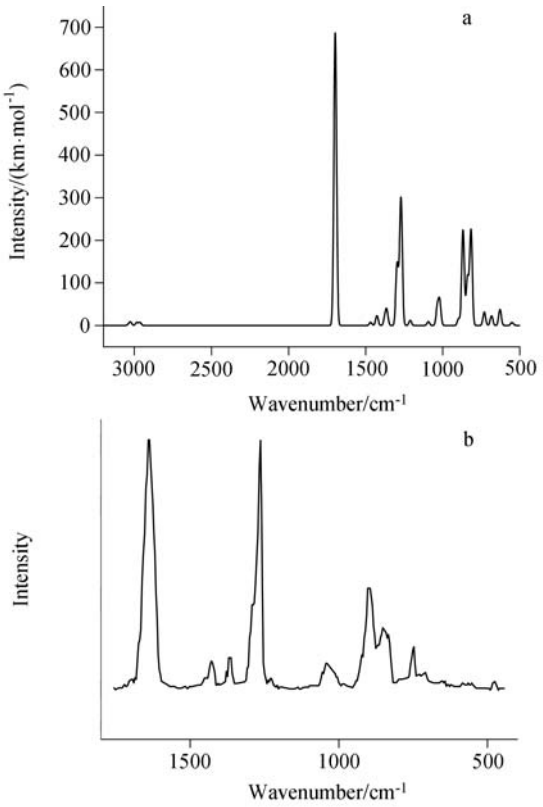

Figure 2 The calculated (a) and experimental (b) infrared spectra for EGDN.

It is evident from Figure 2 that the calculated IR data are all close to the experimental ones. *eg*., there are four very strong IR active modes in the range of 400—1800 cm^{-1}. One is in 1693—1699 cm^{-1} range and is assigned to the NO_2 asymmetric stretching. Another is attributed to the NO_2 symmetry stretching in 1269—1295 cm^{-1}. The third is the range of 1019—1034 cm^{-1}, which corresponds to the C—O symmetry stretching. The forth is less than 1000 cm^{-1}, which mainly corresponds to the O—NO_2 symmetry stretching. All of these prove the reliability of the computational IR. The trivial discrepancy is perhaps due to the intermolecular interactions existing in experimental samples, and at the same time, the theoretical computation aims at the isolated "gas" molecule and is based on the simple harmonic mode.

Based on the above scaled vibrational results, the principle of statistic thermodynamics and self-compiled program, thermodynamic properties ranging from 200 to 800 K were obtained and listed in Table 1, including standard molar heat capacity ($\Delta C_{p,\mathrm{m}}^{\ominus}$), standard molar entropy ($\Delta S_{\mathrm{m}}^{\ominus}$), and standard molar enthalpy ($\Delta H_{\mathrm{m}}^{\ominus}$).

From these data, it is found that all the thermodynamic functions increase with increasing the temperature. This is because the main contributions to the thermodynamic functions are from the translation and rotation of molecules when temperature is low, however, at the higher temperature, the vibrational movement is intensified and, therefore, makes more contributions to the thermodynamic properties, which lead to the increase in the thermodynamic functions. Taking EGDN as an example, the temperature-dependent relations for $\Delta C_{p,\mathrm{m}}^{\ominus}$, $\Delta S_{\mathrm{m}}^{\ominus}$ and $\Delta H_{\mathrm{m}}^{\ominus}$, in the range of 200—800 K can be expressed as follows:

$$\Delta C_{p,\mathrm{m}}^{\ominus}=26.2633+0.4616T-2.2428\times10^{-4}T^2 \quad R^2=0.9999,\ \mathrm{SD}=1.6545 \tag{5}$$

$$\Delta S_{\mathrm{m}}^{\ominus}=261.8054+0.5855T-1.7774\times10^{-4}T^2 \quad R^2=0.9999,\ \mathrm{SD}=2.1036 \tag{6}$$

$$\Delta H_{\mathrm{m}}^{\ominus}=-5.6124+0.0766T+1.1842\times10^{-4}T^2 \quad R^2=0.9998,\ \mathrm{SD}=1.5220 \tag{7}$$

where R^2 and SD are the correlation coefficient and standard deviation, respectively. These equations show good relations between the three thermodynamic functions and temperature. Meanwhile,

$$\mathrm{d}\Delta C_{p,\mathrm{m}}^{\ominus}/\mathrm{d}T=0.4616-4.4856\times10^{-4}T$$

$$\mathrm{d}\Delta S_{\mathrm{m}}^{\ominus}/\mathrm{d}T=0.5855-3.5548\times10^{-4}T$$

$$\mathrm{d}\Delta H_{\mathrm{m}}^{\ominus}/\mathrm{d}T=0.0766+3.3684\times10^{-4}T$$

It is obvious that the gradients of $\Delta C_{p,\mathrm{m}}^{\ominus}$ and $\Delta S_{\mathrm{m}}^{\ominus}$ to the temperature decrease, but that of $\Delta H_{\mathrm{m}}^{\ominus}$ increases, as the temperature increases.

In addition, all the thermodynamic functions in-

Table 1 Thermodynamic properties of the title compounds at different temperatures[a]

Compound		*T*							
		200	298.15	300	400	500	600	700	800
EGDN	$\Delta C^{\ominus}_{p,m}$	110.03	143.41	144.03	175.47	201.56	222.37	238.93	252.25
	$\Delta S^{\ominus}_{m}$	371.00	421.14	422.03	467.88	509.94	548.60	584.17	616.97
	$\Delta H^{\ominus}_{m}$	15.26	27.70	27.96	43.98	62.87	84.11	107.21	131.79
Di-EGDN	$\Delta C^{\ominus}_{p,m}$	151.60	198.68	199.58	246.60	287.07	320.12	346.93	368.84
	$\Delta S^{\ominus}_{m}$	448.34	517.54	518.77	582.74	642.25	697.61	749.04	796.85
	$\Delta H^{\ominus}_{m}$	20.67	37.83	38.20	60.55	87.30	117.71	151.11	186.94
Tri-EGDN	$\Delta C^{\ominus}_{p,m}$	194.35	254.32	255.50	317.77	372.49	417.74	454.77	485.27
	$\Delta S^{\ominus}_{m}$	524.84	613.39	614.96	697.10	774.06	846.11	913.38	976.16
	$\Delta H^{\ominus}_{m}$	26.27	48.23	48.71	77.41	112.00	151.59	195.27	242.32
Tetra-EGDN	$\Delta C^{\ominus}_{p,m}$	236.31	309.81	311.27	389.09	458.17	515.63	562.85	601.89
	$\Delta S^{\ominus}_{m}$	601.84	709.55	711.48	811.79	906.24	995.02	1078.17	1155.96
	$\Delta H^{\ominus}_{m}$	31.57	58.28	58.86	93.92	136.37	185.16	239.16	297.46
Penta-EGDN	$\Delta C^{\ominus}_{p,m}$	281.12	365.98	367.69	460.1	543.19	612.79	670.26	717.93
	$\Delta S^{\ominus}_{m}$	677.51	805.07	807.34	925.86	1037.69	1143.08	1242	1334.7
	$\Delta H^{\ominus}_{m}$	37.92	69.56	70.24	111.66	161.93	219.84	284.08	353.57
Hexa-EGDN	$\Delta C^{\ominus}_{p,m}$	323.01	421.77	423.77	531.65	628.99	710.73	778.37	834.57
	$\Delta S^{\ominus}_{m}$	750.02	896.81	899.43	1036.2	1165.57	1287.7	1402.51	1510.22
	$\Delta H^{\ominus}_{m}$	43.37	79.78	80.56	128.36	186.52	253.64	328.2	408.93

[a] Units: *T*, K; $\Delta C^{\ominus}_{p,m}$: J•mol^{-1}•K^{-1}; $\Delta S^{\ominus}_{m}$: J•mol^{-1}•K^{-1}; $\Delta H^{\ominus}_{m}$: kJ•mol^{-1}.

crease as the number of CH_2CH_2O groups (n=0, 1, 2, 3, 4, 5) increases. There are good linear relations between n and $\Delta C^{\ominus}_{p,m}$, $\Delta S^{\ominus}_{m}$, or $\Delta H^{\ominus}_{m}$, respectively, and the correlation coefficients are all larger than 0.99:

$$\Delta C^{\ominus}_{p,m}=143.10+55.69n \quad (8)$$

$$\Delta S^{\ominus}_{m}=422.22+95.35n \quad (9)$$

$$\Delta H^{\ominus}_{m}=27.45+10.45n \quad (10)$$

One can find that, for the title compounds, $\Delta C^{\ominus}_{p,m}$, $\Delta S^{\ominus}_{m}$ and $\Delta H^{\ominus}_{m}$ increase on an average by 55.69 J•mol^{-1}•K^{-1}, 95.35 J•mol^{-1}•K^{-1} and 10.45 kJ•mol^{-1}, respectively, when one CH_2CH_2O group is added, which shows good group additivity of thermodynamic functions.

We believe that the mentioned equations and data in Table 1 are helpful for the further studies on the other physical, chemical, and explosive properties of the title compounds.

Detonation performance

Table 2 collects V, ρ, D and P of the title compounds. The calculated heats of formation E_{HOF}, oxygen balances OB_{100} and Q are also listed in this Table.

The oxygen balances (OB_{100}) were calculated using the formula (11), which can be used to rudely predict the impact sensitivities of the explosives.[34]

$$OB_{100}=\frac{100(2n_O-n_H-2n_C-2n_{COO})}{M} \quad (11)$$

where n_O, n_H, and n_C represent the numbers of O, H, and C atoms, respectively; n_{COO} is the number of COO, and here n_{COO}=0 for the nitrate esters; M is the molecular weight.

From Table 2, we see that EGDN detonation performances (ρ=1.75 g•cm^{-3}, D=8.96 km•s^{-1}, P=35.03 GPa) are best among the title compounds, and almost better than those of the important explosive, 1,3,5-trinitro-1,3,5-triazacyclohextane (RDX, ρ=1.81 g•cm^{-3}, D=8.75 km•s^{-1}, P=34.70 GPa). On the whole, the energy and density of dinitrate esters decrease as the number of CH_2CH_2O groups (n) increases, which shows that above CH_2CH_2O groups have adverse effects on detonation performance of title compounds with the same number of nitrate groups.

Figure 3 presents the relationships between OB_{100}, E_{HOF}, Q, V, ρ, D or P and the number of CH_2CH_2O groups (n). The correlation equations are: $V=84.89+36.09n$, $E_{HOF}=-240.68-160.65n$, $\rho=1.728-0.106n+0.008n^2$, $P=33.990-8.040n+0.833n^2$, $D=8.861-0.989n+0.091n^2$, $Q=1607.253-194.051n+16.644n^2$, $OB_{100}=2.364-3.286n+0.289n^2$, and the corresponding correlation coefficients are 0.9975, 0.9997, 0.9404, 0.9653, 0.9825, 0.9857 and 0.9847, respectively.

Table 2 Predicted densities and detonation performances of the title compounds

Compound	OB_{100}	Q/(J•g^{-1})	E_{HOF}/(kJ•mol^{-1})	V/(cm^3•mol^{-1})	ρ/(g•cm^{-3})	D/(km•s^{-1})	P/GPa
EGDN	2.63	1622.7	−238.66	86.65	1.75	8.96	35.03
Di-EGDN	−1.02	1409.2	−401.83	123.00	1.59	7.78	24.89
Tri-EGDN	−3.33	1272.4	−566.56	154.42	1.55	7.25	21.23
Tetra-EGDN	−4.39	1184.3	−723.78	188.67	1.51	6.81	18.37
Penta-EGDN	−6.10	1123.9	−875.48	229.35	1.43	6.39	15.58
Hexa-EGDN	−6.99	1035.7	−1047.6	268.61	1.39	6.14	14.08

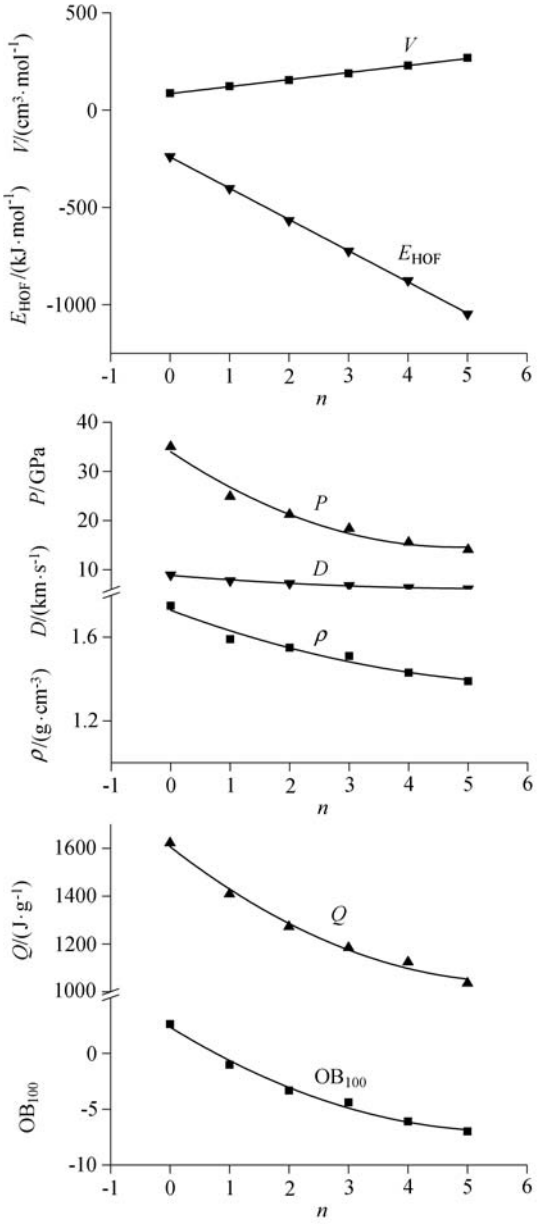

Figure 3 Correlations between OB_{100}, E_{HOF}, Q, V, ρ, D or P and the number of CH_2CH_2O groups (n) for the title compounds.

Pyrolysis mechanism

Bond overlap populations

Bond overlap populations reflect the electron accumulations in the bonding region, and they can provide us detailed information about the chemical bond. As a whole, the less Mulliken bond populations the bond has, the more easily the bond breaks. Though Mulliken population analysis[35] suffers from some shortcomings, such as the basis set dependence, results derived from Mulliken population analysis under the same calculation condition are still meaningful for comparing trends in the electron distribution for homologous compounds as was done here. The bond populations obtained from the Mulliken population analysis for the title compounds at the B3LYP/6-31G* level are listed in Table 3.

Table 3 Mulliken bond populations for the title compounds

Compound	M_{O-NO_2}	M_{C-C}	M_{C-H}	M_{C-O}
EGDN	0.1494	0.3226	0.3501	0.1664
Di-EGDN	0.1518	0.3515	0.3425	0.1610
Tri-EGDN	0.1533	0.3504	0.3414	0.1597
Tetra-EGDN	0.1503	0.3233	0.3416	0.1579
Penta-EGDN	0.1517	0.3542	0.3418	0.1459
Hex-EGDN	0.1532	0.3533	0.3401	0.1581

Inspecting the data in Table 3, it can be found that, for dinitrate ester, the overlap population of the O—NO_2 (M_{O-NO_2}) relatively smaller than those of other bonds, which indicates that the O—NO_2 may be the trigger bond during a thermolysis initiation process.

For the title compounds, comparing EGDN, Di-EGDN and Tri-EGDN, it can be found that with the number of CH_2CH_2O groups increasing, M_{O-NO_2} increases as expected. This suggests that the stability increases and that their sensitivities decrease accordingly, which confirms that the CH_2CH_2O group has an insensitizing effect in this range. Meanwhile, comparing the Tetra-EGDN, Penta-EGDN and Hex-EGDN, the same variation law can be found. However, the M_{O-NO_2} of Tetra-EGDN is less than that of Tri-EGDN, which indicates that in certain n value range the CH_2CH_2O group has an insensitizing effect on dinitrate esters. For the title compounds, the order of the stability is EGDN＜Tetra-EGDN＜Penta-EGDN＜Di-EGDN＜Hex-EGDN＜Tri-EGDN based on the bond overlap populations.

In a word, comparison of bond overlap populations could be primarily used to identify the pyrolysis mechanism, the stability and the relative magnitude of the sensitivity of the homologic energetic materials.

Kinetic parameter

Another main concern for the energetic materials is whether they are kinetically stable enough to be of practical interest. Thus, studies on the bond dissociation or pyrolysis mechanism are important and essential for understanding the decomposition process of the energetic materials, since they are directly relevant to the sensitivity and stability of the energetic compounds. In this paper, for the title compounds, four possible initial steps in the pyrolysis route are considered by breaking following bonds: (1) O—NO_2; (2) C—C; (3) C—H and (4) C—O. It should be pointed out that the weakest O—NO_2, C—O, C—H and C—C bonds are selected as the breaking bonds based on the Mulliken bonding population analyses at the B3LYP/6-31G* level. Table 4 summarizes the computed BDE and BDE_0 values at the B3LYP/6-31G* levels. Compared with BDE_0, BDE parallelly descends 21.9—37.0 kJ/mol, which indicates that using BDE with or without correction for zero-point energy will not have influences on the identification of trigger linkage and pyrolysis mechanism.

Generally speaking, the less the energy is required to break a bond, the weaker the bond is, and the more easily the bond becomes a trigger bond, that is to say, the corresponding compound is more unstable and the sensitivity is larger. Comparing the BDE of the main bonds of the title compounds in Table 4, it can be seen that, BDE of homolysis of the O—NO_2 bond is the least, which suggests that the O—NO_2 bond may be a trigger bond during a thermolysis initiation process. This validates the conclusion drawn from the above Mulliken population analysis and is consistant with experimental conclusion.[36]

Comparing EGDN, Di-EGDN and Tri-EGDN, it can be found that their BDE for the homolysis of O—NO_2 bonds increased gradually, indicating that the substitution of CH_2CH_2O increases the stability and decreases their sensitivities accordingly. Meanwhile, comparison of BDE between Tri-EGDN and Tetra-EGDN shows that, the substitution of CH_2CH_2O decreases their stability and increases sensitivities accordingly. Comparing Tetra-EGDN, Penta-EGDN and Hex-EGDN, it can be found that their BDE for the homolysis of O—NO_2 bonds still increased gradually. This suggests that in some n value range, the introduction of CH_2CH_2O groups increases the stability of the molecules, which validates the above Mulliken population analysis. The order of the stability is EGDN < Tetra-EGDN < Penta-EGDN < Di-EGDN < Hex-EGDN < Tri-EGDN based on the Kinetic parameter analysis.

Conclusion

Using the B3LYP/6-31G* method, we have theoretically studied the structures and the performances for the dinitrate esters, and the conclusions of this work are as follow:

(1) The IR spectra of six dinitrate esters have six characteristic regions which were assigned to the asymmetry and symmetry stretches of C—H, the NO_2 asymmetric stretching, the NO_2 symmetry stretching, the characteristic peaks of ether groups (CH_2CH_2O), the C—O symmetry stretching and the fingerprint regions.

(2) Thermodynamic properties all increase quantitatively with increasing temperature and number of CH_2CH_2O groups. The increments for heat capacities and entropies decrease, while they increase constantly for enthalpies as the temperature increases.

(3) For the dinitrate esters, the oxygen balance, volume, density, detonation velocity and detonation pressure linearly decrease with the increase of the number of CH_2CH_2O groups.

(4) For the title compounds, M_{O-NO_2} and BDE for the rupture of O—NO_2 bond are the least in each molecule, indicating that this bond is the weakest and may be the trigger bond during thermolysis processes. The number of the CH_2CH_2O group has an influence on the stability of the molecules.

(5) The kinetic parameters and the static electronic structural parameters are related with each other, and all can be parallelly or equivalently used to identify the stability and the relative magnitude of impact sensitivity for homologous energetic materials.

Table 4 BDE for main kinds of the bonds (kJ•mol^{-1})

Compound	BDE				BDE_0			
	O—NO_2	C—C	C—H	C—O	O—NO_2	C—C	C—H	C—O
EGDN	140.46	324.24	382.79	303.24	161.53	361.3	421.65	333.70
Di-EGDN	144.00	329.12	375.64	313.69	166.46	359.96	412.47	346.57
Tri-EGDN	145.77	329.53	374.09	315.31	168.29	360.48	410.89	348.14
Tetra-EGDN	140.99	326.61	376.50	314.79	159.89	357.9	412.99	346.57
Penta-EGDN	142.56	328.98	371.25	310.07	165.67	360.22	407.74	346.83
Hex-EGDN	145.72	327.37	373.08	314.01	168.29	358.38	409.13	347.35

[a] BDE_0 denotes the bond dissociation energies without zero-point energy corrections, while BDE denotes the bond dissociation energies including zero-point energy corrections.

Supporting information

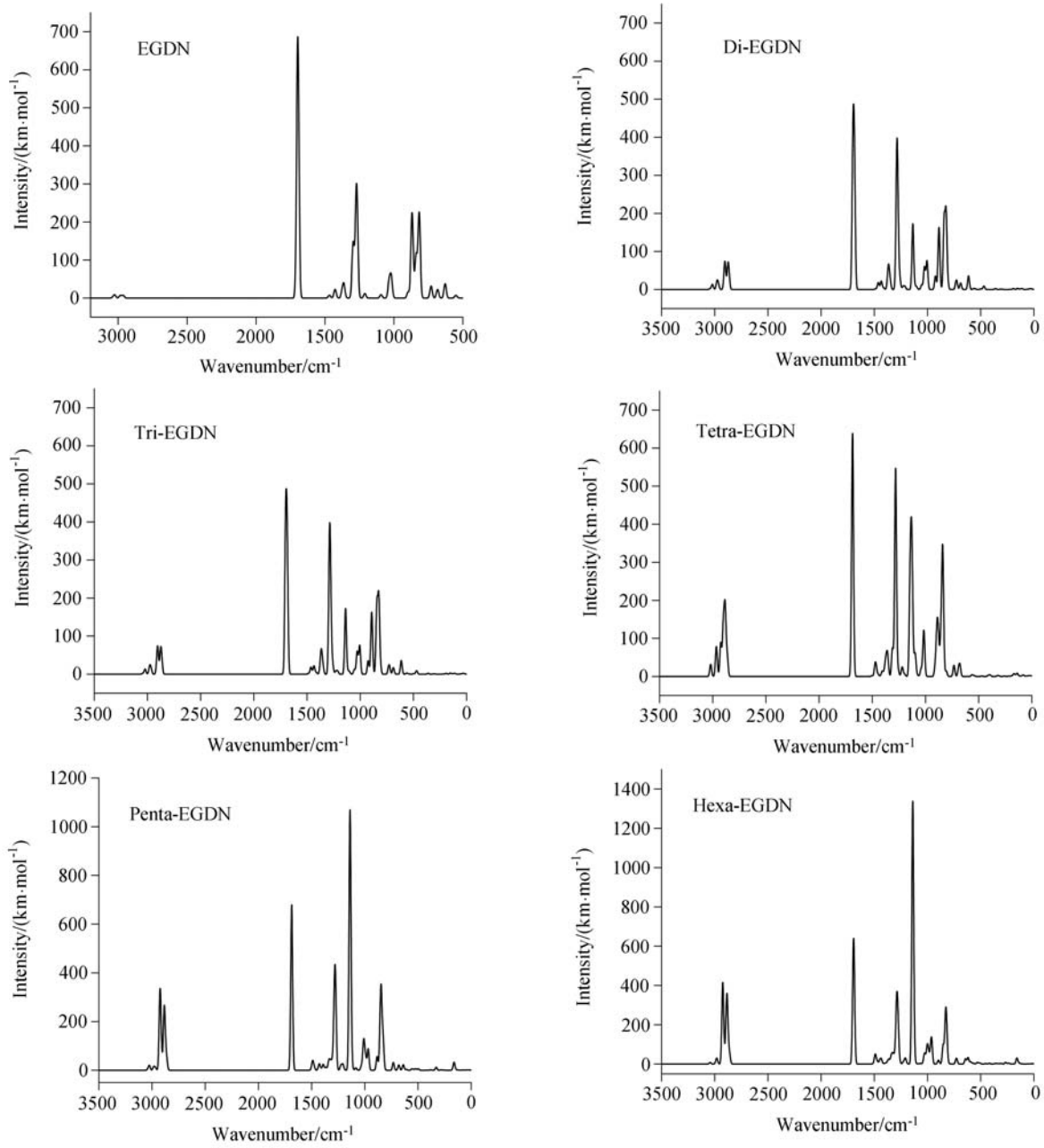

Figure 1S The calculated infrared spectra for the title compounds.

References

1 Perger, W. F.; Zhao, J. J.; Winey, J. M.; Gupta, Y. M. *Chem. Phys. Lett.* **2006**, *428*, 394.
2 Zaoui, A.; Sekkal, W. *Solid State Commun.* **2001**, *118*, 345.
3 Muthurajan, H.; Sivabalan, R.; Talawar, M. B.; Anniyappan, M.; Venugopalan, S. *J. Hazard. Mater.* **2006**, *133*, 30.
4 Agrawal, J. P.; Surve, R. N.; Sonawane, S. H. *J. Hazard. Mater.* **2006**, *77*, 11.
5 Gong, X. D.; Xiao, H. M. *THEOCHEM* **2001**, *572*, 213.
6 Turker, L.; Erkoc, S. *J. Hazar. Mater.* **2006**, *136*, 164.
7 Turker, L. *THEOCHEM* **2005**, *717*, 9.
8 Zeng, X. L.; Chen, W. H.; Liu, J. C.; Kan, J. L. *THEOCHEM* **2007**, *810*, 47.
9 Zeng, X. L.; Chen, W. H.; Liu, J. C. *Acta Phys.-Chim. Sin.* **2007**, *23*, 192.
10 Chen, Z. X.; Xiao, J. M.; Xiao, H. M.; Chiu, Y. N. *J. Phys. Chem. A* **1999**, *103*, 8062.
11 Zhang, J.; Xiao, H. M. *J. Chem. Phys.* **2002**, *116*, 10674.
12 Xu, X. J.; Xiao, H. M.; Ju, X. H.; Gong, X. D.; Zhu, W. H. *J. Phys. Chem. A* **2006**, *110*, 5929.
13 Wang, G. X.; Gong, X. D.; Xiao, H. M. *Chin. J. Chem.* **2008**, *26*, 1357.
14 Lee, C.; Yang, W.; Parr, R. G. *Phys. Rev. B* **1988**, *37*, 785.
15 Becke, A. D. *J. Chem. Phys.* **1992**, *97*, 9173.
16 Hariharan, P. C.; Pople, J. A. *Theor. Chim. Acta* **1973**, *28*, 213.
17 Frisch, M. J.; Trucks, G. W.; Schlegel, H. B.; Scuseria, G.

E.; Robb, M. A.; Cheeseman, J. R.; Montgomery, J. A.; Vreven, J. T.; Kudin, K. N.; Burant, J. C.; Millam, J. M.; Iyengar, S. S.; Tomasi, J.; Barone, V.; Mennucci, B.; Cossi, M.; Scalmani, G.; Rega, N.; Petersson, G. A.; Nakatsuji, H.; Hada, M.; Ehara, M.; Toyota, K.; Fukuda, R.; Hasegawa, J.; Ishida, M.; Nakajima, T.; Honda, Y.; Kitao, O.; Nakai, H.; Klene, M.; Li, X.; Knox, J. E.; Hratchian, H. P.; Cross, J. B.; Adamo, C.; Jaramillo, J.; Gomperts, R.; Stratmann, R. E.; Yazyev, O.; Austin, A. J.; Cammi, R.; Pomelli, C.; Ochterski, J. W.; Ayala, P. Y.; Morokuma, K.; Voth, G. A.; Salvador, P.; Dannenberg, J. J.; Zakrzewski, V. G.; Dapprich, S.; Daniels, A. D.; Strain, M. C.; Farkas, O.; Malick, D. K.; Rabuck, A. D.; Raghavachari, K.; Foresman, J. B.; Ortiz, J. V.; Cui, Q.; Baboul, A. G.; Clifford, S.; Cioslowski, J.; Stefanov, B. B.; Liu, G.; Liashenko, A.; Piskorz, P.; Komaromi, I.; Martin, R. L.; Fox, D. J.; Keith, T.; Al-Laham, M. A.; Peng, C. Y.; Nanayakkara, A.; Challacombe, M.; Gill, P. M. W.; Johnson, B.; Chen, W.; Wong, M. W.; Gonzalez, C.; Pople, J. A., *Gaussian 03*, Gaussian, Inc., Pittsburgh PA, **2003**.

18 Scott, A. P.; Radom, L. *J. Phys. Chem.* **1996**, *100*, 16502.

19 Hill, T. L. *Introduction to Statistic Thermodynamics*, Addison-Wesley, New York, **1960**.

20 Kamlet, M. J.; Jacobs, S. J. *J. Chem. Phys.* **1968**, *48*, 23.

21 Zhang, X. H.; Yun, Z. H., *Explosive Chemistry*, National Defence Industry Press, Beijing, **1989** (in Chinese).

22 Xu, X. J.; Xiao, H. M.; Ju, X. H.; Gong, X. D.; Zhu, W. H. *J. Phys. Chem. A* **2006**, *110*, 5929.

23 Qiu, L.; Xiao, H. M.; Gong, X. D.; Ju, X. H.; Zhu, W. H. *J. Phys. Chem. A* **2006**, *110*, 3797.

24 Xu, X. J.; Xiao, H. M.; Gong, X. D.; Ju, X. H.; Chen, Z. X. *J. Phys. Chem. A* **2005**, *109*, 11268.

25 Stewart, J. J. P. *J. Comput. Chem.* **1989**, *10*, 209.

26 (a) Goh, E. M.; Cho, S. G.; Park, B. S. *J. Def. Technol. Res.* **2000**, *6*, 91.
(b) Dorsett, H.; White, A. Aeronautical and Maritime Research Laboratory, Defence Science and Technology Organization (DSTO), *Technical Report DSTO-GD-0253*, Australia, **2000**.
(c) Sikder, A. K.; Maddala, G.; Agrawal, J. P.; Singh, H. *J. Hazard. Mater.* **2001**, *84*, 1.

27 Stine, J. R. *Los Alamos National Laboratory's Report*, New Mexico, **1981**.

28 Ammon, H. L. *Struct. Chem.* **2001**, *12*, 205.

29 Karfunkel, H. R.; Gdanitz, R. J. *J. Comp. Chem.* **1992**, *13*, 1171.

30 Rice, B. M.; Sorescu, D. C. *J. Phys. Chem. B* **2004**, *108*, 17730.

31 Qiu, L.; Xiao, H. M.; Gong, X. D.; Ju, X. H.; Zhu, W. *J. Hazard. Mater.* **2007**, *141*, 280.

32 Lide, D. R. *CRC* (*Cyclic Redundancy Check*) *Handbook of Chemistry and Physics*, CRC Press LLC, Boca Raton, Florida, **2002**.

33 Beresneva, G. A.; Khristenko, L. V.; Krasnoshchekov, S. V.; Pentin, Y. A. *J. Appl. Spectrosc.* **1988**, *48*, 614.

34 Kamlet, M. J.; Adolph, H. G. *Prop. Explos. Pyrotech.* **1979**, *4*, 30.

35 Dong, H. S.; Zhou, F. F. *High Energy Explosives and Their Corresponding Performance*, Science Press, Beijing, **1989** (in Chinese).

36 Ou, Y. X. *Explos. Mater. Sci.*, Beijing University of Science and Technology Press, Beijing, **2006** (in Chinese).

(E0901143 Ding, W.)